from the same slice, but without a window in the electrode, and find that I_{th} increases by $\approx 5\%$ in 5 kbar, i.e., $I_{th}^{-1}\, dI_{th}/dP = +0.01\ \text{kbar}^{-1}$. The increase in spontaneous current for a loss-free laser is[6]

$$\frac{1}{J_{spon}}\frac{dJ_{spon}}{dP} = \frac{2}{E_g}\frac{dE_g}{dP} \approx 0.017\ \text{kbar}^{-1}, \tag{7}$$

which is about twice that observed above. The increase of τ_{nr} with pressure suggests that the internal efficiency increases with pressure, and this should reduce the overall increase of I_{th} with pressure. We can estimate this effect as follows:

If we write $J_{th} = \eta_i^{-1} J_{spon}$, then

$$\frac{1}{J_{th}}\frac{dJ_{th}}{dP} = \eta_i \frac{d}{dP}(\eta_i^{-1}) + \frac{1}{J_{spon}}\frac{dJ_{spon}}{dP}, \tag{8}$$

and writing $\eta_i = 1 + (\tau_r/\tau_{nr})$, then, taking $\tau_r = 3.5$ ns and neglecting its pressure dependence, our data for τ_{nr} gives

$$\eta_i \frac{d}{dP}(\eta_i^{-1}) \approx -0.09,$$

and so Eqs. (7) and (8) predict

$$\frac{1}{J_{th}}\frac{dJ_{th}}{dP} = +0.017 - 0.09 = -0.07\ \text{kbar}^{-1}.$$

In other words, the increase in τ_{nr} implies such a large improvement in η_i that J_{th} should actually decrease with pressure. The discrepancy with our observed increase of I_{th} cannot be resolved by making other reasonable estimates of τ_r or its possible pressure dependence, and so the increase of I_{th} with P is, in fact, much greater than we expect from our measurements of τ_{nr}.

Since the η^{-1} vs $1/\sqrt{L}$ plot is only used over its linear portion, which extends to $\sim 0.5\, I_{th}$, we postulate that there is some further nonlinear loss mechanism at threshold which does not contribute in the current range used to measure τ_{nr} and which causes I_{th} to increase with P. It is known that the energy separations of the Γ, L, and X conduction-band minima decrease with increasing P, and so we postulate that thermal transfer of carriers to the L minimum in the active region or to the X or L minima or DX centers in the cladding regions could be responsible for our observed increase of I_{th}.

In summary, we have measured the linear losses in a GaAs DH laser at high injection and as a function of hydrostatic pressure. We find that the nonradiative lifetime increases with pressure, suggestive of capture at a deep state by multiphonon emission, but despite the improvement this implies in the internal quantum efficiency, we also observed that the threshold current increases with pressure. We postulate that this is caused by nonlinear losses which are effective at threshold, such as carrier transfer to higher conduction-band minima in the active cladding region.

We thank K. Woodbridge and P. J. Hulyer for growth of the structure and fabrication of the devices, respectively.

[1] C. van Opdorp and G. W.'t Hooft, J. Appl. Phys. **52**, 3827 (1981).
[2] S. M. Sze, *Physics of Semiconductor Devices*, 2nd ed. (Wiley, New York, 1981), p. 35, Eq. (58).
[3] P. Blood and J. J. Harris, J. Appl. Phys. **56**, 993 (1984).
[4] D. V. Lang and R. A. Logan, J. Electron. Mater. **4**, 1053 (1975).
[5] C. E. Barnes and G. A. Samara, Appl. Phys. Lett. **43**, 677 (1983).
[6] D. Patel, A. R. Adams, P. D. Greene, and G. D. Henshall, Electron. Lett. **18**, 527 (1982).

Structural development during mechanical alloying of crystalline niobium and tin powders

M. S. Kim and C. C. Koch
Department of Materials Science and Engineering, North Carolina State University, Raleigh, North Carolina 27695-7907

(Received 26 February 1987; accepted for publication 9 July 1987)

The structural development with milling time during mechanical alloying of niobium and tin powders, of average composition Nb_3Sn, was followed by x-ray diffraction. The elemental powders initially alloy mechanically to form an A15 structure phase. With continued milling, the A15 phase transforms to an amorphous structure. The kinetics of the structure changes are dependent on the milling media and atmosphere. The measured lattice parameter a_0 for the A15 phase prepared with tungsten carbide milling media in an argon atmosphere agrees with the literature value of a_0 for bulk Nb_3Sn. However, milling with steel media introduced significant contamination by iron and an anamolous expansion of the A15 phase lattice. Amorphization of the A15 phase is believed to be due to the creation of a critical defect concentration by the mechanical deformation.

In recent years, there has been interest in the formation of amorphous metallic alloys by solid-state reactions. The current understanding of this phenomenon has been reviewed by Schwarz.[1] Mechanical alloying is one of the solid-state methods which has been used to synthesize a number of amorphous alloys.[2–6] Mechanical alloying (MA) is a high-energy ball milling technique for producing composite metal powders with controlled microstructures by the repeated cold welding and fracture of powder particles.[7] If MA is continued to the point where the starting powders are mixed

 0021-8979/87/203450-04$02.40

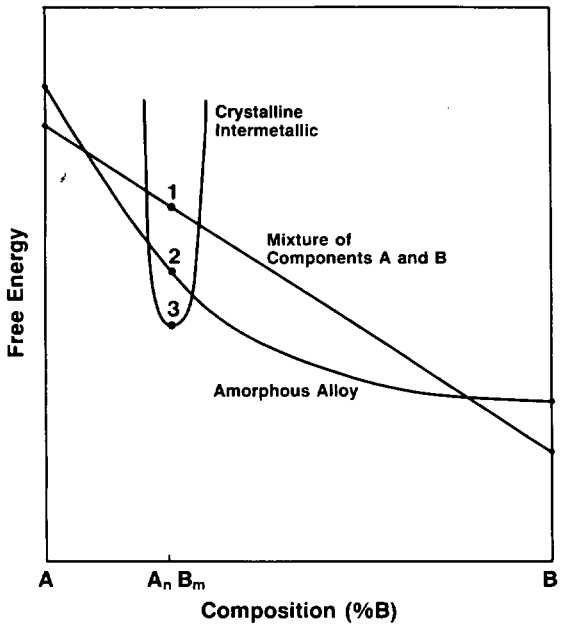

FIG. 1. Schematic free energy vs composition curves for (1) the mixture of crystalline components, (2) the amorphous alloy, and (3) the crystalline intermetallic compound.

to dimensions of a few atomic spacings, then an alloy of the elemental powders can be formed. Depending on the alloy system, this alloy might be the equilibrium phase (solid solution or intermediate phase), a metastable crystalline phase, or an amorphous structure. Schwarz and Koch[8] have demonstrated that the amorphous structure can be obtained by starting either with powder of the pure elemental components or with powder of the equilibrium intermetallic compound. The mechanism(s) of amorphization by mechanical alloying can be discussed in terms of the free energy versus composition curves, shown schematically in Fig. 1. State [1] represents the free energy of the mixture of pure crystalline A and B powders, state [2] the free energy of the amorphous phase treated as an undercooled liquid[3] with a large negative heat of mixing, and state [3] the free energy of the equilibrium phase $A_N B_M$. For many glass-forming binary systems, such as Ni-Nb[2,9] and Ni-Ti,[3] it is believed that amorphization occurs by solid-state interdiffusion of the components such that the free energy is lowered from [1] to [2]. This has been observed in systems with large negative heats of mixing. Starting with pure elemental powder of the components has resulted in this sequence in the amorphization experiments reported up to now. It is assumed in this case that the kinetics for formation of the amorphous phase are more rapid than for the formation of the equilibrium intermetallic compound. It has also been shown that the amorphous structure can be attained if one mills powder of the equilibrium intermetallic compound.[8] In this case, the free energy must be raised from state [3] to state [2]. It was suggested[10] that this could be accomplished by raising the free energy of the crystalline compound by introduction of defects during mechanical milling, in analogy to amorphization by energetic particle irradiation.[11] In this note we describe experiments in which amorphization occurs in the Nb-Sn system by the path [1] → [3] → [2]. That is, mechanical alloying of the elemental Nb and Sn powders first produces the crystalline A15 compound, which, after continued milling, transforms to the amorphous structure.

Elemental powders of nominal purity (99.8% for Nb, 99.5% for Sn) of starting diameter $< 45\,\mu$m were blended in the desired proportions for mechanical alloying. Mechanical alloying was carried out in a SPEX Mixer/Mill Model 8000. The vials and milling media consisted of either hardened tool steel (5.7×7.6 cm) with 440C martensitic stainless-steel balls (7.9 mm diam) or a tungsten carbide-cobalt vial (5.7×6.35 cm) and balls (7.9 and 11.1 mm^2 diam). The vial atmospheres during MA were nominally either air or argon. Several ball-to-powder weight ratios were used (4:1, 6:1, and 8:1).

During mechanical alloying the vials were opened periodically for removal of small amounts of powder for analysis. X-ray diffraction (XRD) measurements were made on

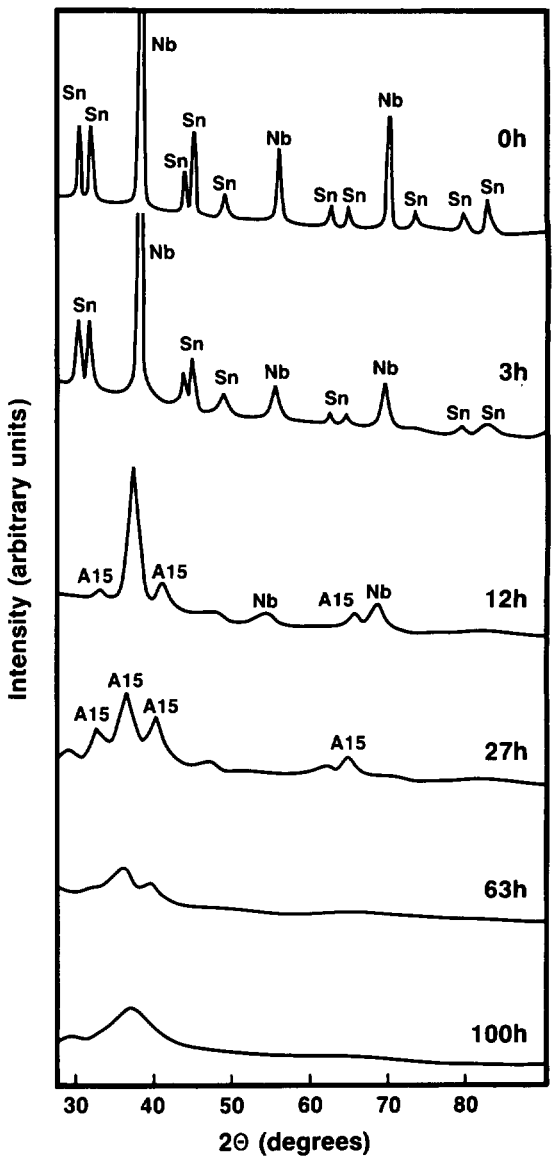

FIG. 2. Diffraction Patterns of Nb-25 at. % Sn powder milled in argon with steel media. Milling times 0, 3, 12, 27, 63, and 100 h.

the powder in either a Debye–Scherrer camera or on an XRD-5 diffractometer, both with CuK_α radiation. The peak positions of the most intense diffraction maxima [(110) Nb, (210) A15, or first maxima of the amorphous pattern] were measured. The Scherrer relation was used to obtain a semiquantitative measure of the degree of disorder being introduced by mechanical alloying. The effective scattering length d determined from the breadth of an x-ray diffraction line is given by

$$d = 0.9\lambda / \beta \cos\theta,$$

where θ is the scattering angle for x rays of wavelength λ, and β is the full width at half maximum of the diffraction line. In the derivation of the Scherrer relation, d is the average dimension of crystallites normal to the x-ray scattering vector. We refer to d as an effective scattering length and roughly view it as a distance over which long range atomic periodicity is lost.

After mechanical alloying, chemical analysis was performed on portions of the powders removed from the vial. Oxygen analyses were made by Wah Chang Teledyne Corp.[12] and metallic analyses by an electron beam microprobe at NCSU. After mechanical alloying for long periods (>20 h) in air, large oxygen concentrations were measured in the Nb-Sn powder [2.0 wt. % (11.3 at. %) to 4.7 wt. % (23.3 at. %)]. After milling for long times (>50 h) samples loaded in an argon glove box, the oxygen content was found to be 0.8 wt. % (4.8 at. %) to 1.3 wt. % (7.6 at. %), somewhat greater than in the as-received powders; 0.4 wt. % (2.4 at. %) to 0.6 wt. % (3.6 at. %). While the oxygen concentrations are high, at least for the samples loaded in argon, they are not at the level of oxides. The nominal bulk compositions of Nb and Sn were confirmed by the electron microprobe.

A sequence of x-ray diffraction intensities are presented in Fig. 2 for Nb - 25 at. % Sn powder loaded under argon and mechanically alloyed for times from 0 to 100 h with the steel milling media. After mechanical alloying (MA) for 3 h all the diffraction lines for bcc Nb and tetragonal Sn are still apparent, although broadened. After 12 h of MA the (200), (210), (211), and (321) lines of the A15 Nb_3Sn structure are observed in the forward reflection region. The (210) A15 line may also contain intensity of the remaining Nb (110) line, since residual intensity of the second strongest Nb line, (211), is still observed. After 27 h of MA the intensities of the A15 (200) and (211) lines have increased relative to the (210) line and the remaining resolvable Nb (211) has decreased considerably. After 63 h of MA no Nb lines are visible and only small remnants of the A15 lines are visible above the broad diffraction maximum typical of an amorphous structure. After 100-h MA the diffraction pattern shows mainly the broad maximum of an amorphous structure.

The kinetics of the structural development in Nb -25 at. % Sn by MA were a function of the milling media and the environment. The effective scattering length d calculated from the width of the most intense diffraction line by the Scherrer relation, and the shift in peak position, 2θ, of this line, can be used to follow the MA kinetics. These data are listed in Table I.

The structural development with milling time was not homogeneous. That is, at a given time a mixture of phases was present. The sequence of structures with milling time were as follows: first, elemental powders + A15 phase; then elemental powder + A15 phase + amorphous structure; then A15 + amorphous; and finally, mainly amorphous.

The lattice parameter for the A15 phase was calculated from the measured peak positions of the strongest lines; (200), (210), (211), and (321). The calculated lattice parameter for the samples milled under argon with tungsten carbide media was 0.529 ± 0.001 nm, in excellent agreement with literature values for bulk A15 Nb_3Sn,[13] in spite of the significant line broadening. The powder milled under argon with the steel media, however, exhibited expanded lattice

TABLE I. Structural changes as a function of milling time for Nb-25 at. % Sn powder.

Milling conditions	Milling time (h)	2θ (deg) for maximum diffraction peak	Effective scattering length d (nm)	Observed phases
Argon	4	38.3	7.65	Nb, Sn
Tungsten carbide	16	37.8	6.0	Nb, Sn, A15
	22.5	37.8	5.25	A15
	58	37.8	3.5	A15, Amorph.
	104	37.8	2.33	Amorph., A15
	150	37.2	1.39	Amorph.
	170	37.2	1.16	Amorph.
Argon	3	38.4	12.4	Nb, Sn
Steel	12	37.8	6.37	Nb, A15
	27	37.0	3.50	A15, Amorph.
	63	36.8	1.55	Amorph., A15
	100	37.1	1.04	Amorph.
Air	1	38.4	13.9	Nb, Sn
Steel	6	38.2	5.87	Nb, A15
	15	37.8	3.01	A15, Amorph.
	20	37.4	1.40	Amorph.

parameters with $a_0 = 0.531 \pm 0.001$ nm after 12 h of milling and $a_0 = 0.541 \pm 0.002$ nm after 27 h. The oxygen levels in both sets of samples milled under argon were comparable; however, the samples milled with the steel balls and vial contained significant quantities of iron impurities, incorporated from the milling media. Iron concentrations measured by electron microprobe analysis were 2.0 at. % after 12 h of milling and 4.6 at. % after 27 h. We conclude that iron is responsible for the observed increase in a_0. This apparent expansion of the lattice of Nb_3Sn by iron incorporated by mechanical alloying is in contrast to the results of Caton,[14] who measured a contraction of the A15 Nb_3Sn lattice with iron additions from 0.5291 nm (0% Fe) to 0.5278 nm (5 at. % Fe) in sintered material. This latter result is consistent with the smaller atomic radius of iron (0.127 nm) compared to Nb (0.147 nm) and Sn (0.155 nm).[15] Since it seems clear that the incorporation of iron is responsible for the observed lattice expansion of the A15 phase in our mechanically alloyed Nb_3Sn, we conclude that the iron must be present in the Nb_3Sn lattice in a nonequilibrium, perhaps interstitial, arrangement.

The significant line broadening of the A15 structure Bragg maxima suggests a high defect concentration introduced by mechanical alloying. In turn, this implies the occurrence of extensive plastic deformation in nominally brittle A15 Nb_3Sn under the stress/strain conditions existing during mechanical alloying. The evidence for a highly defected A15 structure is consistent with our hypothesis[10] that amorphization of intermetallics by mechanical alloying occurs when the defects introduced raise the free energy of the crystalline intermetallic to that of the amorphous state.

In summary, mechanical alloying of pure crystalline niobium and tin mixtures, at the Nb_3Sn composition, has been carried out as a function of milling time. A heavily cold-worked crystalline A15 phase forms initially and eventually transforms to the amorphous state.

This research was sponsored by the National Science Foundation under NSF Grant No. DMR-8318561.

[1]R. B. Schwarz, Mater. Res. Soc. Bull. **XI** (3), 55 (1986).
[2]C. C. Koch, O. B. Cavin, C. G. McKamey, and J. O. Scarbrough, Appl. Phys. Lett. **43**, 1017 (1983).
[3]R. B. Schwarz, R. R. Petrich, and C. K. Saw, J. Non-Cryst. Solids **76**, 281 (1985).
[4]E. Hellstern and L. Schultz, Appl. Phys. Lett. **48**, 124 (1986).
[5]C. Politis and W. L. Johnson, J. Appl. Phys. **60**, 1147 (1986).
[6]C. Politis, Physica **135B**, 286 (1985).
[7]J. S. Benjamin, Sci. Am. **234**, 40 (1976).
[8]R. B. Schwarz and C. C. Koch, Appl. Phys. Lett. **49**, 146 (1986).
[9]P. Y. Lee and C. C. Koch, J. Non-Cryst. Solids (in press).
[10]C. C. Koch and M. S. Kim, J. Phys. (Paris) **46**, C8-573 (1985).
[11]M. L. Swanson, J. R. Parsons, and C. W. Hoelke, Radiat. Eff. **9**, 249 (1971).
[12]Teledyne Wah Chang Albany, Analytical Lab., 1600 Old Salem Road N.E., Albany, Oregon.
[13]P. Villars and L. D. Calvert, Eds., *Pearson's Handbook of Crystallographic Data for Intermetallic Phases* (American Society for Metals, Metals Park, OH, 1985), Vol. 3, p. 2836.
[14]R. Caton, J. Less Common Metals **109**, 9 (1985).
[15]W. B. Pearson, *The Crystal Chemistry and Physics of Metals and Alloys* (Wiley-Interscience, New York, 1972), p.151.

Negative differential resistance in a strained-layer quantum-well structure with a bound state

G. S. Lee, K. Y. Hsieh, and R. M. Kolbas
Department of Electrical and Computer Engineering, North Carolina State University, Raleigh, North Carolina 27695-7911

(Received 16 February 1987; accepted for publication 17 June 1987)

Strained-layer resonant tunneling structures of pseudomorphic GaAs-AlAs-$In_{0.09}Ga_{0.91}As$-AlAs-GaAs are studied both experimentally and with a simple quantum mechanical model. The energy spectrum of the unbiased structure includes the usual resonant states and also bound states due to the narrow-band gap InGaAs well. Strong tunneling (and negative differential resistance) are observed for the resonant states. We observe for the first time tunneling associated with a "bound-state" energy level which result in a zero differential conductance feature. Qualitative agreement between the experimental and calculated results are shown.

Negative differential resistance (NDR) in double-barrier quantum-well structures[1] has been investigated for high-frequency devices[2–5] and to understand the tunneling mechanisms, Fabry–Perot[1] or sequential.[6,7] There have been a number of experimental[8–12] and theoretical[13–16] works on the study of resonant tunneling transport in lattice-matched AlGaAs-GaAs and AlAs-GaAs double-barrier structures. With respect to other material systems negative differential resistance in double-barrier resonant structures of strained-layer GaAsP-GaAs (Ref. 17) and multiquantum wells of lattice-matched AlInAs-GaInAs (Ref. 7) has been reported at cryogenic temperatures. In a previous paper[18] and in Ref. 19 it is pointed out that the resonant tunneling voltages can be adjusted by varying the depth of the InGaAs well in an AlGaAs-InGaAs strained-layer double-barrier structure, while holding constant all other thickness and composition

 0021-8979/87/203453-04$02.40